JEM

Journal of Electron Microscopy **60(5)**: 337–351 (2011)
doi: 10.1093/jmicro/dfr052

Biological: Full-length

Structome of *Saccharomyces cerevisiae* determined by freeze-substitution and serial ultrathin-sectioning electron microscopy

Masashi Yamaguchi[1,*], Yuichi Namiki[1], Hitoshi Okada[1,2], Yuko Mori[3], Hiromitsu Furukawa[3], Jinfang Wang[4], Misako Ohkusu[1] and Susumu Kawamoto[1]

[1]Medical Mycology Research Center, Chiba University, 1-8-1 Inohana, Chuo-ku, Chiba 260-8673, Japan, [2]Non-Profit Organization, Integrated Imaging Research Support, Villa Royal Hirakawa 103, 1-7-5 Hirakawa-cho, Chiyoda-ku, Tokyo 102-0093, Japan, [3]System in Frontier Inc., 2-8-3 Shinsuzuharu Bldg. 4F, Akebono-cho, Tachikawa-shi, Tokyo 190-0012, Japan and [4]Department of Mathematics and Informatics, Graduate School of Science, Chiba University, 1-33 Yayoi-cho, Inage-ku, Chiba 263-8522, Japan
*To whom correspondence should be addressed. E-mail: yama@faculty.chiba-u.jp

Abstract The cell structure has been studied using light and electron microscopies for centuries, and it is assumed that the whole structure is clarified by now. Little quantitative and three-dimensional analysis of cell structure, however, has been undertaken. We have coined a new word, 'structome', by combining 'structure' and '-ome', and defined it as the 'quantitative and three-dimensional structural information of a whole cell at the electron microscopic level'. In the present study, we performed structome analysis of *Saccharomyces cerevisiae*, one of the most widely researched biological materials, by using freeze-substitution and serial ultrathin-sectioning electron microscopy. Our analysis revealed that there were one to three mitochondria, ~220 000 ribosomes in a cell, and 13–28 endoplasmic reticula/Golgi apparatus which do not form networks in the cytoplasm in the G1 phase. Nucleus occupied ~10.5% of the cell volume; cell wall occupied ~17%; vacuole occupied ~5.8%; cytoplasm occupied ~64%; and mitochondria occupied only ~1.7% in the G1 phase. Structome analysis of cells would form a base for the post-genome research.

Keywords structome, *Saccharomyces cerevisiae*, freeze-substitution, serial ultrathin sectioning, 3D, reconstruction, ultrastructure

Received 6 May 2011, accepted 17 June 2011; online 9 September 2011

Introduction

The number of cells that makes up the human body is $\sim 6 \times 10^{13}$ cells, and the human brain consists of $\sim 1.5 \times 10^{10}$ cells. However, it is not known, for example, how many ribosomes are there in a single yeast cell, nor how much volume endoplasmic reticula occupy and how they localize within a cell. The word 'structome' was coined by combining 'structure' and '-ome', and defined as the 'quantitative three-dimensional structural information of a whole cell at the electron microscopic level' [1].

Three-dimensional analysis of cell components such as mitochondria has been performed using serial ultrathin-sectioning electron microscopy since 1969 [2]. The report that mitochondria, which appeared as multiple entities, were in fact connected to each other as a single unit was a big

surprise to cell biologists [3]. Although there have been studies using three-dimensional analysis on specific components by electron microscopy [4–7], there were no 3D analysis on all cell components. In 2003, we performed structome analysis of *Exophiala dermatitidis* yeast cells for the first time [8], and found that: (i) there are ~200 000 ribosomes, 17–52 mitochondria, 5–10 endoplasmic reticula in a cell; (ii) mitochondria occupied ~10%, nucleus ~7%, cell wall ~22%, cytosol ~48% and only 0.2% endoplasmic reticula of the cell volume; (iii) there is no giant mitochondrion in this species; (iv) membranes are classified into three groups, namely plasma membrane–vacuole, nuclear envelope–endoplasmic reticulum (ER)–mitochondria and autophagosomes [8].

Saccharomyces cerevisiae strain S288c was used for the first genome analysis in eukaryotes [9] and is one of the most common materials studied in cell biology worldwide. Since genetic, biochemical and morphological information on this material has accumulated, structural information on the whole cell in this strain at the electron microscopic level, i.e. the structome, would be useful additional information. Here, we report the structome of *S. cerevisiae* strain S288c determined by freeze-substitution and serial ultrathin-sectioning electron microscopy.

Materials and methods

Organism and culture conditions

Saccharomyces cerevisiae strain S288c was kindly provided by Dr. Takayuki Mizuno at Tokushima Bunri University, Japan. Cells were cultured in 20 ml of YPD liquid medium (1% yeast extract, 2% polypeptone and 2% glucose) in a 100-ml Erlenmeyer flask at 30°C with reciprocal shaking at 120 rpm [10]. Exponentially growing cells (OD_{660} was ~1.0) were used for structome analysis.

Specimen preparation and electron microscopy

Detailed methods are described previously [10]. Briefly, cells were sandwiched between two copper disks and snap frozen by plunging into propane/isopentane mixture cooled with liquid nitrogen. They were freeze substituted in acetone containing 2% osmium tetroxide at –80°C, and embedded in epoxy resin (Quetol-812, Nisshin EM, Tokyo). Serial ultrathin sections were cut to a thickness of 90 nm with a diamond knife, picked up on two-slit grids and stained with uranyl acetate and lead citrate [11]. The grids were then set in a multi-specimen holder (MSH-400, JEOL Datum, Tokyo), and micrographic images were taken on FG films (Fujifilm Corp., Tokyo) at a magnification of 10 000× in a JEM 1200EX electron microscope (JEOL, Tokyo, Japan) at 80 kV. Complete series of thin sections through whole cells were composed of 31–49 sections, which is fewer than the previous report [12], because cells were cut parallel to the long axis of the cell [10].

For morphological observation and measurements of membrane thickness of various cell components (see Fig. 1, Tables 3 and 4), 50-nm thick sections were cut, mounted on 400-mesh grids, stained with uranyl acetate and lead citrate, covered with Super support film (Nisshin EM, Ltd., Tokyo, Japan) and photographed at 20 000–40 000× magnifications.

Three-dimensional reconstruction of cells

Micrographs printed at a magnification of 20 000× were digitized by a flat-bed scanner to a resolution of 300 dots per 25.4 mm. Each digitized micrograph was stacked by using the software called Stack 'N' Viz (System in Frontier, Inc., Tokyo, Japan). Cell components of cell wall, nucleus, mitochondria, vacuole, small vesicles and virus-like particles were specified separately. Three-dimensional images of each cell component were combined to construct whole cell images. Finally, they were subjected to smoothing.

Enumeration and measurement of various cell components

Number of mitochondria, vacuoles and ER/Golgi were counted in the 3D reconstructed images (Fig. 2). Length and diameter of various components and membrane thickness were measured on electron micrographs of 20 000–100 000× magnifications using a 10× loupe with a 0.1-mm scale when necessary. Cell wall thickness was measured at the minor axis of cells. Ribosome particles were enumerated on electron micrographs of 100 000×

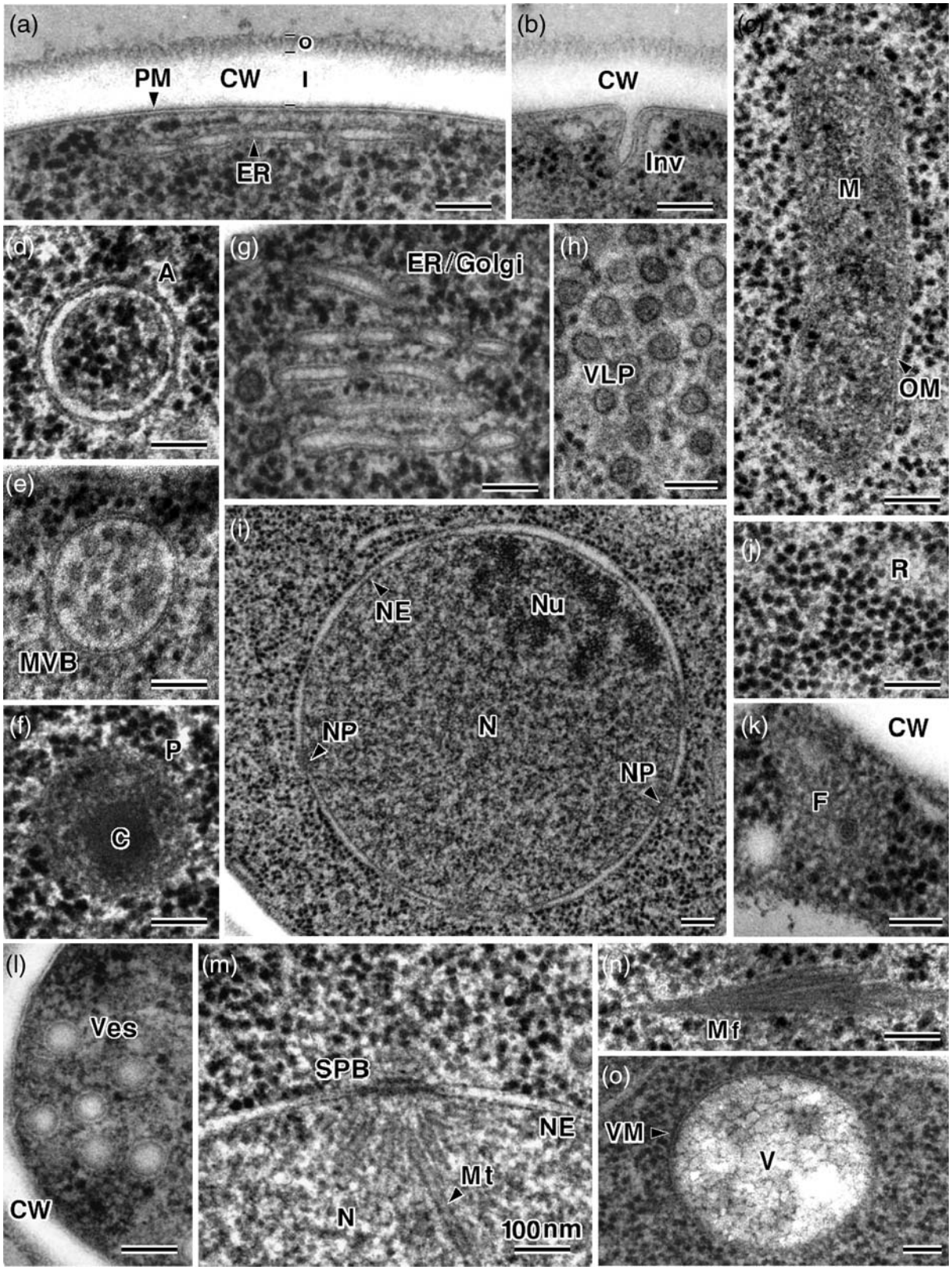

Fig. 1. High magnification images of various cell components in *S. cerevisiae.* (a) The cell wall (CW) and plasma membrane (PM). O, outer cell wall layer; I, inner cell wall layer. ER, endoplasmic reticulum. (b) Invagination (Inv). (c) Mitochondrion (M) with outer membrane (OM). (d) Autophagosome (A). (e) Multivesicular body (MVB). (f) Peroxisome (P) with a crystal (C). (g) ER/Golgi apparatus (ER/Golgi). (h) Virus-like particles (VLP). (i) Nucleus (N), nuclear envelope (NE), nuclear pore (NP) and nucleolus (Nu). (j) Ribosomes (R). (k) Filasome (F). (l) Small vesicles (Ves). (m) Spindle pole body (SPB) and Microtubule (Mt). (n) Microfilaments (Mf). (o) Vacuole (V) with vacuolar membrane (VM). All figures are of the same magnification except (i) and (o). Bar = 100 nm.

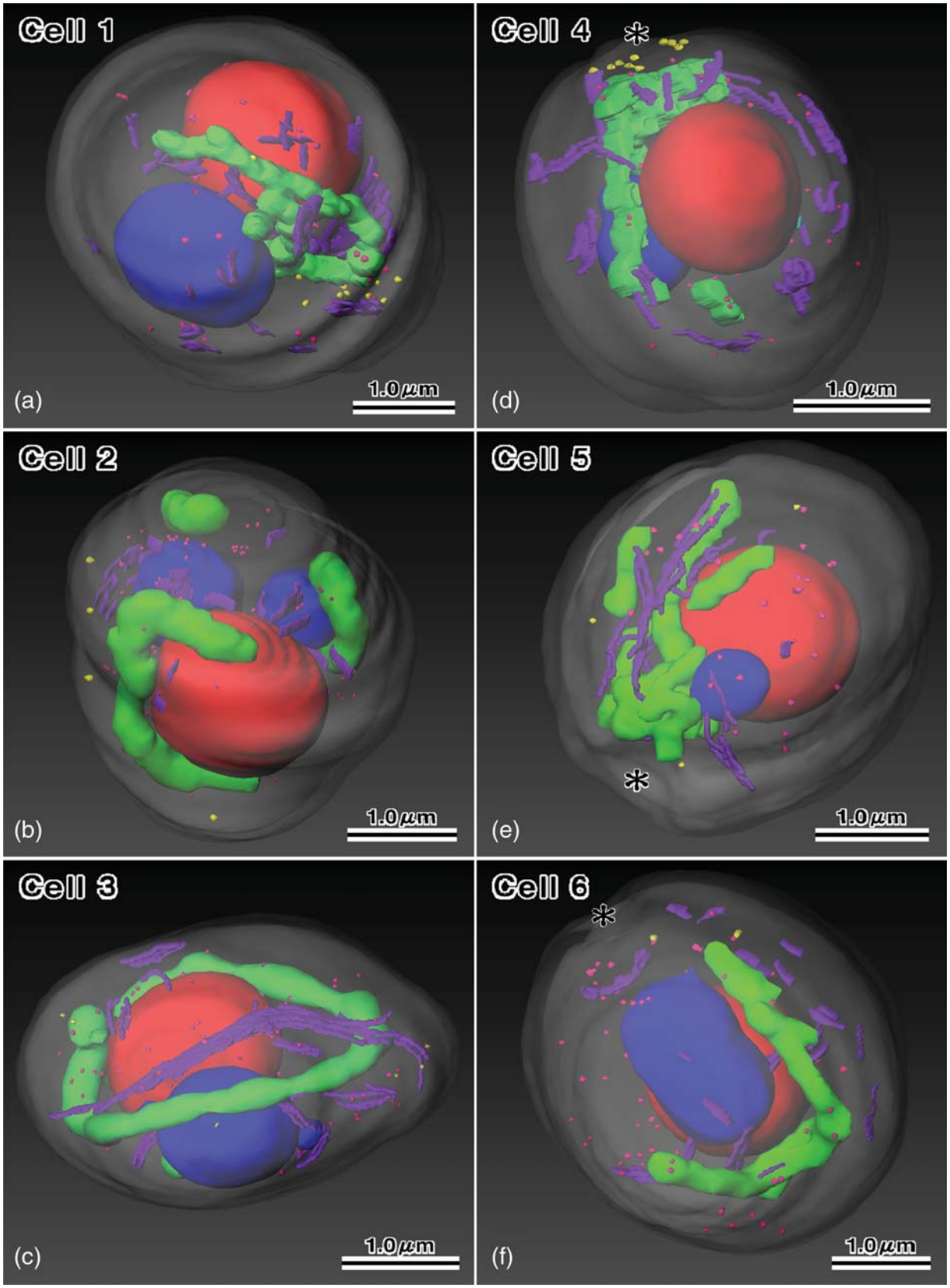

Fig. 2. Three-dimensional reconstructions of *S. cerevisiae* Cells 1–6. Cells 1–3 are in the G1 phase, and Cells 4–6 are in the early G1 phase. Red, nucleus; green, mitochondria; blue, vacuoles; purple, endoplasmic reticula/Golgi apparatus; yellow points, small vesicles; red points, virus-like particles; * in Cells 4–6, position where mother cell attaches. For movies, see the supplementary data online.

magnification in a limited area of the cytosol. The number of ribosome particles per cubic micrometer was calculated by multiplying the area examined by section thickness (90 nm). Then the number of ribosomes in a cell was determined by multiplying the number per unit volume by the cytosol volume.

Statistical analysis

Differences between the G1 phase (Cells 1–3) and the early G1 phase (Cells 4–6) in numbers of various organelles and components were analyzed by Student's *t*-test. Differences between the G1 phase and the early G1 phase in volumes of cells and cell components and between Cells 1 and 5 in distances between ERs/Golgi apparatus and mitochondria were also analyzed by *t*-test. Whether distances between small vesicles and plasma membrane were different from random distribution were analyzed statistically, assuming that the cytoplasm was ellipsoid with major axis of 3.58 µm and minor axis of 2.97 µm (the major axis was determined by subtracting cell wall thickness and plasma membrane thickness from cell length: $3.85 - 0.12 \times 2 - 0.016 \times 2 = 3.58$; minor axis: $3.24 - 0.12 \times 2 - 0.016 \times 2 = 2.97$). The detailed analytical procedure is described in Appendix.

Results

A total of 2642 micrographs were taken for the present study. Thirty-two complete serial sections of *S. cerevisiae* cells were photographed and six cells were chosen and analyzed for structome analysis. Three cells were single unbudded cells (G1 phase), and the other three were daughter cells that finished cytokinesis but were still attached to mother cells (cells soon after cytokinesis, early G1 phase).

Quality of cell images

Figure 1 shows high magnification images of various cell components in *S. cerevisiae* S288c strain prepared by freeze-substitution fixation. Cell wall consisted of outer fibrous layer and inner electron-transparent layer (Fig. 1a). Plasma membrane, ER/Golgi membrane (Fig. 1a and g), mitochondrial outer membrane (Fig. 1c), membranes of autophagosome (Fig. 1d) and multivesicular body (Fig. 1e), nuclear envelopes (Fig. 1m) and vacuolar membrane (Fig. 1o) showed tri-lamellar structures whose inner and outer leaflets were electron dense and whose middle leaflet was electron transparent. The near-spherical shape of the nucleus (Fig. 1i) was consistent with images observed by light microscopy, confirming that the cells were not subject to any artificial force during specimen preparation. These observations showed that structures of the cells in this study were in their natural state and in high resolution, conditions that are essential for structome analysis.

Tables 1 and 2 show the numbers and volumes of various organelles and cell components in the

Table 1. Numbers of various organelles and cell components in individual *S. cerevisiae* cells

	G1 phase				Early G1 phase				Difference between A and B: *P*-value by *t*-test
Organells/components	**Cell 1**	**Cell 2**	**Cell 3**	**Mean ± SD (A)**	**Cell 4**	**Cell 5**	**Cell 6**	**Mean ± SD (B)**	
Nucleus	1	1	1	1.0 ± 0.0	1	1	1	1.0 ± 0.0	–
Nucleolus	1	1	1	1.0 ± 0.0	1	1	1	1.0 ± 0.0	–
Spindle pole body	1	1	1	1.0 ± 0.0	1	1	1	1.0 ± 0.0	–
Mitochondria	1	3	3	2.3 ± 1.2	2	4	1	2.3 ± 1.5	> 0.05
ERs/Golgi apparatus	28	24	13	21.7 ± 7.8	16	14	24	18.0 ± 5.3	> 0.05
Vacuoles	1	1	4	2.0 ± 1.7	2	1	2	1.7 ± 0.6	> 0.05
Autophagosomes	0	0	1	0.3 ± 0.6	2	1	2	1.7 ± 0.6	< 0.05 ($t = 2.83$)
Multivesicular bodies	0	5	0	1.7 ± 2.9	0	0	0	0.0 ± 0.0	> 0.05
Ribosomes	195 000	272 000	183 000	217 000 ± 48 000	170 000	115 000	239 000	175 000 ± 62 000	> 0.05
Ribosomes/µm^3	19 100	20 200	19 400	19 600 ± 600	17 700	20 000	20 600	19 400 ± 1500	> 0.05
Small vesicles	17	6	6	9.7 ± 6.4	11	3	2	5.3 ± 4.9	> 0.05
Filasomes	22	40	26	29.3 ± 9.5	22	22	18	20.7 ± 2.3	> 0.05
Virus-like particles	39	109	100	82.7 ± 38.1	46	53	75	58.0 ± 15.1	> 0.05
Peroxisomes	0	0	0	0.0 ± 0.0	0	0	0	0.0 ± 0.0	–
Invaginations	20	45	30	31.7 ± 12.6	6	37	25	22.7 ± 15.6	> 0.05

Table 2. Volumetric measurement of *S. cerevisiae* cells and cell components

	G1 phase				Early G1 phase				Difference between A and B : *P*-value by *t*-test
Cell/organelles	Cell 1	Cell 2	Cell 3	Mean ± SD (A)	Cell 4	Cell 5	Cell 6	Mean ± SD (B)	
Cell	15.9[a]	20.7	14.8	17.1 ± 3.1	13.4	8.9	17.5	13.3 ± 4.3	>0.05
	(100)[b]	(100)	(100)	(100 ± 0)	(100)	(100)	(100)	(100 ± 0)	(–)
Cell wall	2.3	3.5	2.9	2.9 ± 0.6	2.2	1.9	3.0	2.4 ± 0.6	>0.05
	(15)	(17)	(19)	(17 ± 2)	(16)	(22)	(17)	(18 ± 3)	(>0.05)
Nucleus	1.8	2.2	1.4	1.8 ± 0.4	1.3	0.9	1.6	1.3 ± 0.4	>0.05
	(11.5)	(10.5)	(9.5)	(10.5 ± 1.0)	(9.8)	(9.9)	(9.4)	(9.7 ± 0.3)	(>0.05)
Nucleolus	0.43	0.49	0.29	0.40 ± 0.10	0.17	0.06	0.44	0.22 ± 0.19	>0.05
	[23.5][c]	[22.3]	[20.5]	[22.1 ± 1.5]	[13.1]	[7.1]	[26.8]	[15.7 ± 10.1]	(>0.05)
Mitochondria	0.32	0.27	0.27	0.28 ± 0.03	0.12	0.18	0.20	0.17 ± 0.04	<0.05 (t = 4.13)
	(2.0)	(1.3)	(1.8)	(1.7 ± 0.4)	(1.0)	(2.1)	(1.1)	(1.4 ± 0.6)	(>0.05)
ERs/Golgi apparatus	0.16	0.07	0.13	0.12 ± 0.04	0.07	0.04	0.06	0.06 ± 0.02	>0.05
	(1.0)	(0.4)	(0.9)	(0.7 ± 0.3)	(0.5)	(0.4)	(0.4)	(0.5 ± 0.1)	(>0.05)
Vacuoles	1.05	1.24	0.69	0.99 ± 0.28	0.12	0.07	0.88	0.36 ± 0.45	>0.05
	(6.6)	(6.0)	(4.7)	(5.8 ± 1.0)	(1.0)	(0.8)	(5.0)	(2.2 ± 2.4)	(>0.05)
Autophagosomes	0	0	0.01	0.004 ± 0.007	0.003	0.001	0.02	0.006 ± 0.008	>0.05
	(0)	(0)	(0.08)	(0.03 ± 0.05)	(0.02)	(0.006)	(0.09)	(0.04 ± 0.04)	(>0.05)
Multivesicular bodies	0	0.02	0	0.008 ± 0.014	0	0	0	0 ± 0	>0.05
	(0)	(0.11)	(0)	(0.04 ± 0.06)	(0)	(0)	(0)	(0 ± 0)	(>0.05)
Cytosol	10.2[d]	13.5	9.4	11.0 ± 2.2	9.6	5.8	11.7	9.0 ± 3.0	>0.05
	(64)	(65)	(64)	(64 ± 1)	(72)	(65)	(67)	(68 ± 3)	(>0.05)

[a]Volumes were measured in μm^3.
[b]Values between parentheses are percentages of cell volume.
[c]Values between square brackets are percentages of nuclear volume.
[d]The volume of cytosol includes the volume of ribosomes, small vesicles, filasomes and virus-like particles.

Table 3. Length and diameter of *S. cerevisiae* cell and various components (mean ± SD)

Cell components	Length	Diameter	Number measured
Cell	3.85 ± 0.48 μm	3.24 ± 0.42 μm	36
Nucleus		1.63 ± 0.20 μm	36
Nuclear pores		94 ± 12 nm	20
Spindle pole body		117 ± 19 nm	8
Mitochondria		230 ± 30 nm	20
Vacuoles	930 ± 490 nm	870 ± 460 nm	47
Autophagosomes	316 ± 77 nm	263 ± 67 nm	25
Multivesicular bodies	206 ± 43 nm	186 ± 39 nm	16
Microvesicles in multivesicular bodies		39 ± 6 nm	14
Ribosomes		20 ± 1 nm	50
Small vesicles		70 ± 6 nm	20
Filasomes		175 ± 33 nm	33
Virus-like particle		52 ± 6 nm	100
Microtubules		25.1 ± 0.5 nm	24
Microfilaments		7.3 ± 0.8 nm	7

six cells. Table 3 shows the length and diameter of cells and various cell components. Table 4 shows the thickness of membranes of various organelles. Three-dimensional reconstructions of Cells 1–6 are shown in Fig. 2. For movies of Fig. 2, see the supplementary data online. Figure 3 shows the ratios of cytosol, cell wall, nucleus, mitochondria, vacuoles and other cell components in six individual cells. Figure 4 shows the average ratios of cytosol, cell wall, nucleus, mitochondria, vacuoles and other cell components in three G1 phase cells. Volume distributions of individual mitochondrion in six cells are shown in Fig. 5. Volume ratios of vacuoles in six cells are shown in Fig. 6. Table 5 shows the analysis of distances between ERs/Golgi apparatus and mitochondria in Cells 1 and 5. Table 6 shows the analysis of distances between small vesicles and plasma membranes in the six cells.

The structome data of *S. cerevisiae* collected using electron micrographs (Fig. 1), 3D reconstruction images (Fig. 2) and quantitative data (Tables 1–6 and Figs. 3–6) were collectively analyzed, and the results are described subsequently.

Table 4. Membrane thickness of various organelles in *S. cerevisiae* (mean ± SD)

Organelle	Total thickness (nm)	Outer leaflet (nm)	Middle leaflet (nm)	Inner leaflet (nm)	Number measured
Plasma membrane	15.6 ± 2.1	4.6 ± 1.0	3.8 ± 0.6	7.3 ± 1.9	20
Vacuole	19.4 ± 2.7	7.8 ± 2.2	4.1 ± 0.8	7.6 ± 1.7	20
Autophagosome	16.8 ± 2.3				11
Multivesicular body	16.9 ± 2.6				8
Nuclear outer envelope	12.6 ± 1.5				20
Nuclear inner envelope	13.3 ± 1.6				20
ER/Golgi apparatus	14.2 ± 1.8				20
Mitochondrial outer membrane	14.1 ± 2.0				20

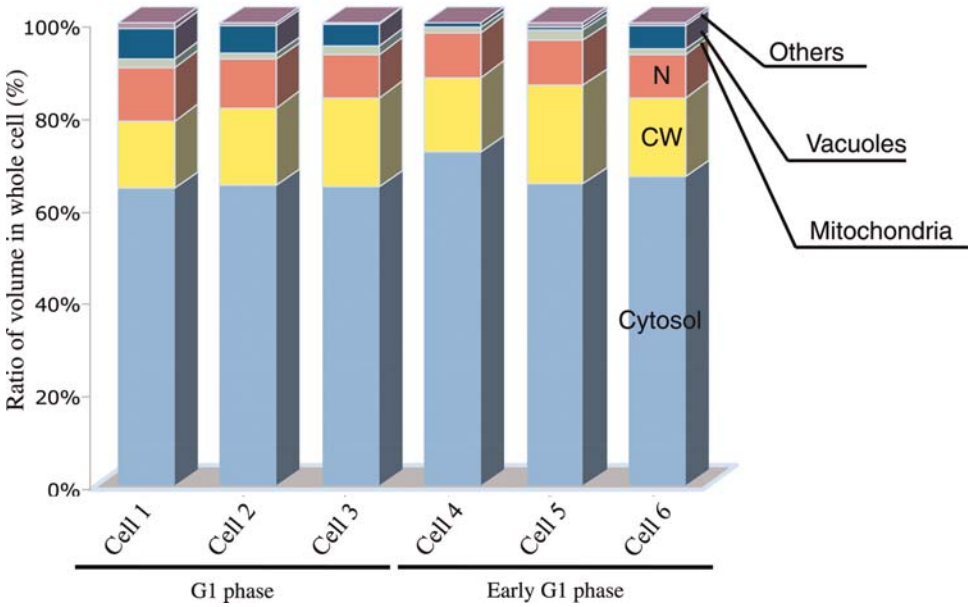

Fig. 3. Proportions of the cytosol (C), cell wall (CW), nucleus (N), mitochondria, vacuoles and other cell components in Cells 1–6. Schematic representation of Table 2. Values are expressed as percent to the cell volume. 'Others' include ER/Golgi apparatus, autophagosomes and multivesicular bodies. The volume of cytosol includes the volume of ribosome particles, small vesicles, filasomes and virus-like particles.

Structome of *S. cerevisiae* in the G1 phase (Cells 1–3)

The cell

The size of *S. cerevisiae* G1 phase cell was ~3.9 µm in length and ~3.2 µm in diameter (Table 3). The volume of the G1 phase cell was ~17.1 µm^3 (Table 2).

The cell wall

The cell wall of *S. cerevisiae* was 120 ± 14 nm thick (average ± standard deviation, 20 measurements) and consisted of two layers (Fig. 1a). The outer cell wall layer was 34 ± 3 nm thick and composed of fibrous materials (Fig. 1a) made of mannoproteins [13,14]. The inner layer was electron transparent, 86 ± 14 nm thick, and made of β-glucan and chitin [14]. The volume of cell wall was ~2.9 µm^3 and constituted 17% of the cell volume (Table 2).

The nucleus, nuclear envelope, nuclear pore and nucleolus

The nucleus was enclosed by a double-layered nuclear envelope (Fig. 1i). The nucleus in interphase cell was spherical (Fig. 1i), ~1.6 µm in diameter (Table 3) and ~1.8 µm^3 in volume, occupying ~10.5% of the cell volume (Table 2, Fig. 4). The nuclear envelope consisted of the outer and inner envelopes. Both measured ~13 nm in thickness (Table 4). The nuclear pore was ~94 nm in

diameter (Table 3) and is known to function in the transport of substances between the nucleoplasm and cytoplasm [15]. There was only one nucleolus in a nucleus (Table 1). The nucleolus was composed of densely packed granular materials (Fig. 1i) ~0.4 μm^3 in volume and occupied ~22% of the nuclear volume (Table 2).

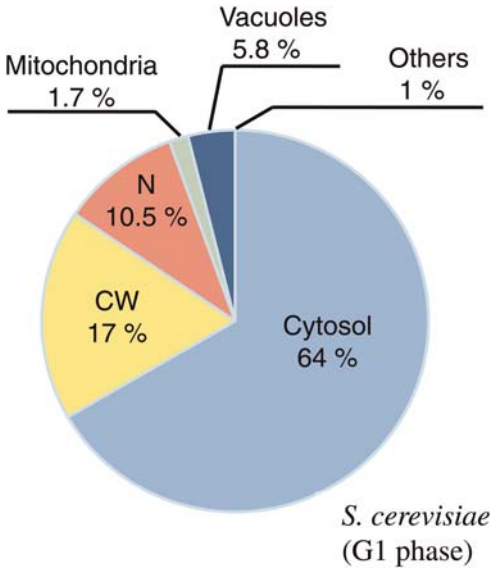

Fig. 4. Average proportions of the cytosol (C), cell wall (CW), nucleus (N), mitochondria, vacuoles and other cell components in *S. cerevisiae* G1 phase cells (Cells 1–3). Sixty-four percent of the cell was occupied by cytosol. Cell wall occupied 17%, nucleus occupied 10.5%, mitochondria occupied 1.7%, and vacuole occupied 5.8% of the cell volume.

The mitochondria

The mitochondria appeared oval or elongated in ultrathin sections (Fig. 1c) and were found to be string-shaped and sometimes branched in 3D reconstruction images (Fig. 2). The mitochondria had a cross-sectional diameter of ~230 nm (Table 3) and a length of up to 6.2 μm (Fig. 2c). The mitochondria in a cell had a total volume of ~0.28 μm^3 and occupied ~1.7% of the cell volume (Table 2, Fig. 4). The volume distributions of individual mitochondrion in Cells 1–3 are shown in Fig. 5. There were one to

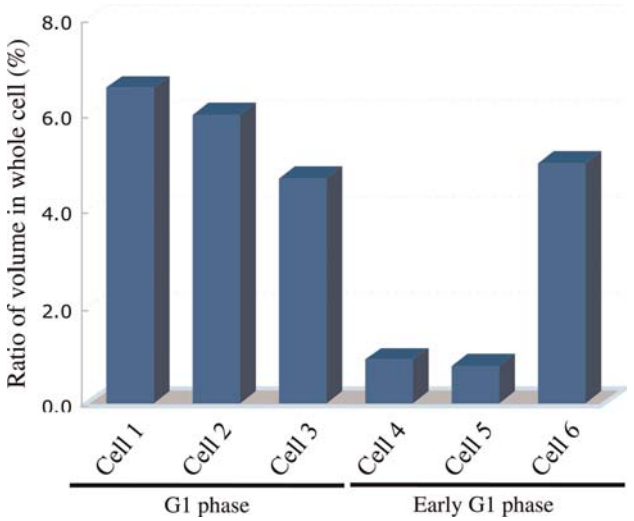

Fig. 6. Volume distributions of vacuoles in six cells. Cells 4 and 5 in the early G1 phase contain less volume than Cells 1–3 in the G1 phase.

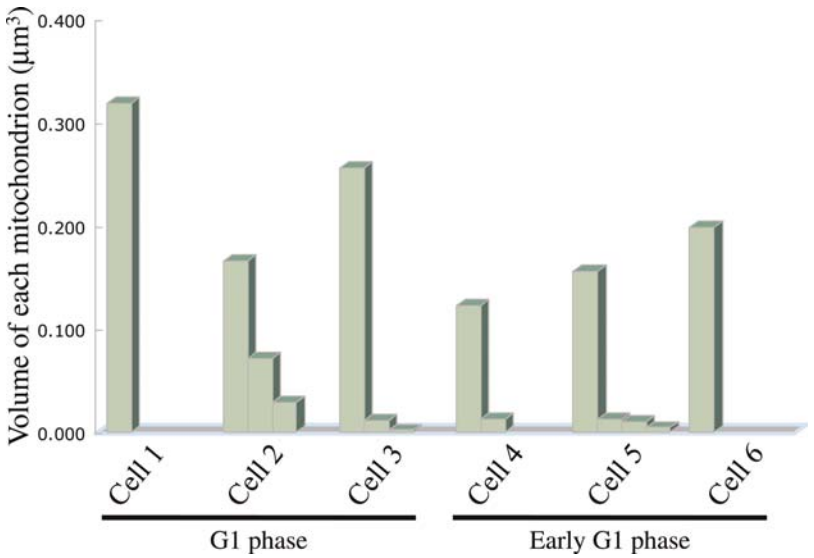

Fig. 5. Volume distributions of individual mitochondrion in six cells. There were one to three mitochondria in G1 phase cells and one to four mitochondria in early G1 phase cells. One giant mitochondrion is present in each cell.

Table 5. Distances between ER/Golgi apparatus and mitochondria in Cells 1 and 5 (see Cells 1 and 5 in Fig. 2)

	G1 phase Cell 1	Early G1 phase Cell 5	Difference between A and B : *P*-value by *t*-test
Number measured	28	14	
≤200 nm (frequency)	19% (A)	71% (B)	$p < 0.001$ ($t = 4.36$)
>200 nm (frequency)	81%	29%	

three mitochondria in a cell, and we found one giant mitochondrion [12] in each cell (Fig. 5).

The mitochondrion was surrounded by an outer membrane, but cristae were not very clear in our culture condition (Fig. 1c). The mitochondrial outer membrane was ~14 nm thick (Table 4).

The ER and Golgi apparatus

In *S. cerevisiae*, Golgi apparatus rarely shows a stacked structure and exists primarily as individual cisternae throughout the cytoplasm [16]. Therefore, we analyzed ER and Golgi apparatus as one organelle (ER/Golgi, see Fig. 1g). Thirteen to twenty-eight ER/Golgi were present in a cell (Table 1), had a total volume of 0.12 μm^3 and occupied ~0.7% of the cell volume (Table 2). Membranes of ER/Golgi measured ~14 nm thick (Table 4).

Vacuoles, autophagosomes and multivesicular bodies

There were one to four vacuoles in a cell (Table 1). Vacuoles were usually spherical (Fig. 1o) with an average diameter of 0.9 μm (Table 3). The total vacuolar volume in a cell was 0.7–1.2 μm^3 and occupied 5–7% of the cell volume (Table 2, Fig. 3). The volume distributions of individual vacuoles in Cells 1–3 are shown in Fig. 6. Vacuolar membrane was ~19 nm thick and consisted of three leaflets with the inner leaflet and the outer leaflet having similar thickness (Table 4).

Autophagosomes (Fig. 1d) were membrane-bound structures in the cytoplasm [17] and had an average length and diameter of 316 and 263 nm, respectively (Table 3). They contained ribosome particles that might be in the process of digestion (Fig. 1d). They were sometimes absent in a cell (Table 1). Their membranes consisted of three leaflets (Fig. 1d) and had a thickness of 17 nm (Table 4). The autophagosome is believed to be the precursor of the autophagic body in the vacuole [17].

Multivesicular bodies were spherical membrane-bound organelles containing microvesicles (Fig. 1e) [18,19]. These microvesicles were ~39 nm in diameter (Table 3). Up to five multivesicular bodies were present in a cell (Table 1), having an average length and diameter of 206 and 186 nm, respectively (Table 3). The membrane of multivesicular body measured ~17 nm in thickness (Table 4) and consisted of three leaflets (Fig. 1e). Thus, membranes of autophagosomes, multivesicular bodies and vacuoles were very similar, suggesting that they have a common origin. Multivesicular bodies are considered to be part of the lysosomal system because they contain acid phosphatase [18].

Ribosomes and cytosol

Ribosomes appeared as electron dense particles of ~20 nm in diameter size (Fig. 1j, Table 3). They were dispersed randomly throughout the cytoplasm. Many were found attached to the ER as well as the outer nuclear envelope. We enumerated the total number of ribosome particles in *S. cerevisiae* cells; the number ranged from 183 000 to 272 000 (Table 1). The number per unit volume of cytosol, however, was relatively constant at ~20 000/μm^3 (Table 1).

The volume of cytosol was calculated by subtracting the volume of all organelles and cell components (from cell wall to multivesicular bodies, but not nucleolus, in Table 2) from the cell volume. Cytosol occupied ~64% of the cell volume (Table 2, Fig. 4).

Table 6. Distances between small vesicles and plasma membranes (see yellow points in Cells 1–6 in Fig. 2)

	G1 phase			Early G1 phase			1–6 cells	
	Cell 1	Cell 2	Cell 3	Cell 4	Cell 5	Cell 6	Total	Mean ± SD
Number measured	17	6	6	11	3	2	45	
Distance (nm)	200 ± 213	165 ± 76	208 ± 71	50 ± 24	108 ± 32	170 ± 5		150 ± 60 ($p < 2.2 \times 10^{-16}$)

Small vesicles and filasomes

Small vesicles were spherical, with clear circumference, had diameters of 70 ± 6 nm and were often found in the cytoplasm near cell walls (Figs. 1l and 2, Table 3) [19]. There were 6–17 of them in a cell (Table 1). They contain glucanase activity [20].

Filasomes were spherical, had diameters of 175 ± 33 nm and consisted of a single microvesicle surrounded by fine filaments (Fig. 1k, Table 3) [7,18]. There were 22–40 filasomes in a cell (Table 1), and often found in the cytoplasm near cell walls.

The spindle pole body, microtubules and microfilaments

Figure 1m shows the spindle pole bodies (SPBs) of interphase cells. The SPB was located within a nuclear envelope and consisted of disk elements with cytoplasmic and nuclear microtubules [21]. The disk elements measured ~117 nm in diameter (Table 3).

Microtubules (Fig. 1m) had a diameter of ~25 nm (Table 3). Most microtubules were associated with the SPB and few were found in the cytoplasm. Microfilaments (Fig. 1n) were of ~7 nm thick (Table 3).

Peroxisomes and virus-like particles

Peroxisomes were observed as electron-dense spherical organelles enclosed by a membrane (Fig. 1f) [22]. They sometimes contained more electron-dense crystal-like structure (Fig. 1f). There were few peroxisomes in cells grown under our culture conditions, and none were found in Cells 1–3 (Table 1).

Virus-like particles were spherical with electron-lucent centers (Fig. 1h) [23] and had a diameter of ~52 nm (Table 3). There were 39–109 particles in a cell (Table 1). The virus-like particles is known to have reverse transcriptase activity [24].

The plasma membrane and membrane systems

The plasma membrane was ~15.6 nm thick and consisted of three leaflets (Fig. 1a, Table 4). The outer leaflet was electron dense, the middle leaflet was electron transparent and the inner leaflet was electron dense. They measured ~4.6, 3.8 and 7.3 nm, respectively (Table 4). The plasma membrane was invaginated into cytoplasm in certain places (Fig. 1b). There were 20–45 invaginations in each cell (Table 1).

Membranes of *S. cerevisiae* might be classified into two groups according to their thickness. The first group had a thickness of 16–19 nm (Table 4) and included the plasma membrane (Fig. 1a), vacuolar membrane (Fig. 1o), membranes of autophagosomes (Fig. 1d) and multivesicular body (Fig. 1e). The second group had a thickness of 13–14 nm (Table 4) and included the outer and inner nuclear envelope (Fig. 1m), ER/Golgi membranes (Fig. 1a and g) and mitochondrial outer membrane (Fig. 1c).

Individual variation among cells

The proportions of cytosol, cell wall, nucleus, mitochondria and vacuoles in Cells 1–3 are shown in Fig. 3. There were little variations in proportions of each organelle among cells.

Structome of *S. cerevisiae* in the early G1 phase (Cells 4–6)

The cell

The volume of the early G1 phase cell was ~13.3 μm^3 (Table 2).

The cell wall

The volume of cell wall was ~2.4 μm^3 and constituted 18% of the cell volume (Table 2).

The nucleus, nuclear envelope, nuclear pore and nucleolus

The nucleus was ~1.3 μm^3 in volume and occupied ~10% of the cell volume (Table 2, Fig. 3), whereas the nucleolus was ~0.2 μm^3 in volume and occupied ~16% of the nuclear volume (Table 2).

The mitochondria

The mitochondria in this stage had a total volume of ~0.17 μm^3 and occupied ~1.4% of the cell volume (Table 2, Fig. 3). The volume distributions of individual mitochondrion in Cells 4–6 are shown in Fig. 5. There were one to four mitochondria, one of which was a giant mitochondrion [12].

The ER and Golgi apparatus

Fourteen to twenty-four ER/Golgi were present in a cell (Table 1) and had ~0.06 μm^3 of total volume, which occupied ~0.5% of the cell volume (Table 2).

Vacuoles, autophagosomes and multivesicular bodies

There were one to two vacuoles in a cell (Table 1). The total vacuolar volume in this stage was 0.1–0.9 μm^3 and occupied 1–5% of the cell volume (Table 2, Fig. 3). The ratio of total vacuolar volume in Cell 4–6 is shown in Fig. 6. One or two autophagosomes were present in this stage (Table 1) and occupied 0.01–0.1% of cell volume (Table 2). There were no multivesicular bodies in this stage (Table 1).

Ribosomes and cytosol

There were 115 000–239 000 ribosome particles in this stage (Table 1). The number per unit volume of cytosol was ~20 000/μm^3 (Table 1). Cytosol occupied ~68% of the cell volume (Table 2).

Small vesicles, filasomes and virus-like particles

There were 2–11 small vesicles, 18–22 filasomes and 46–75 virus-like particles in a cell in this stage (Table 1).

Comparison between structomes of the G1 phase and early G1 phase cells

The total volume of mitochondria was significantly less in the early G1 phase cells than in the G1 phase cells. But, the proportions of mitochondrial volume against whole cell in each stage were not significantly different (Table 2). It may be natural to suppose that the similar proportion of mitochondria as other organelles was transferred into the daughter cell during cell division. Sizes of cells, volumes of cell walls, nucleus, nucleolus, ER/Golgi, vacuoles and cytosols also tended to be smaller in early G1 phase cells than that in G1 phase cells (Table 2), although values were not statistically significant. This is understandable since the daughter cells are usually smaller than the mother cells. The difference in numbers of autophagosomes between G1 phase cells and early G1 phase cells showed a statistical significance (Table 1); this difference may not be truly significant, however, because the *P*-value is close to 5% and the one significant case found could have been produced only by a chance from the 30 cases we analyzed (i.e. if you analyze 20 cases, one case becomes significant only by chance.) The ratios of the vacuolar volume were noticeably smaller in early G1 phase cells (Cells 4–5) than those in G1 phase cells (Cells 1–3) (Fig. 6). These results show that structome dynamics have an interesting relationship to the cell cycle; this aspect of the study is now being further pursued in our laboratory.

Analysis of distances between ER/Golgi and mitochondria

Three-dimensional reconstruction of cells enabled us to measure distances between ER/Golgi and mitochondria in each cell in three dimensions. We determined the proportion of cases having distances ≤200 nm and those having >200 nm. In Cell 1 in the G1 phase, there were fewer cases in which the distance between ER/Golgi and mitochondria were ≤200 nm (19%), whereas there were more cases in which the distance between ER/Golgi and mitochondria were ≤200 nm (71%) in Cell 5 of the early G1 phase, and this difference was found to be statistically significant (Table 5). The same tendency of having mitochondria positioned closer to ER/Golgi in early G1 phase cells than those in G1 phase cells was observed (data not shown), although it was not statistically significant. It can be assumed that a higher energy supply would be necessary in early G1 phase cells than those in G1 phase cells, resulting in a closer association between ER/Golgi and mitochondria in the former. A similar analysis was undertaken in acinar cells of pancreas in mouse [25] in which a closer association between mitochondria and Golgi apparatus was observed, explaining energy supply requirements for the production of secretory granules.

Analysis of distances between small vesicles and plasma membrane

We also measured the distances between small vesicles and plasma membrane in three dimensions in six cells, and found that small vesicles located near the plasma membrane had an average distance of 150 nm from the plasma membrane (Table 6). The value was highly significant (*P*-value was $<2.2 \times 10^{-16}$, see Appendix for detailed statistical analysis) and was not contradicted with the report that small vesicles carry glucanase for cell wall synthesis [20].

Discussion

Generation of autophagosomes, multivesicular bodies and peroxisomes

Autophagosomes were not found in two of the six cells examined, multivesicular bodies were not found in five cells and no peroxisomes were found in all six cells examined (Table 1). The presence of cells that have none of these organelles means that these organelles may not always be necessary for the cell to live and that they could be generated *de novo* in the cytoplasm when necessary.

Number and volume of mitochondria

In contrast to a previous report [3], there were more than one mitochondrion in early G1 and G1 phases in *S. cerevisiae* (Table 1 and Fig. 5). Stevens [12] found that there is a close relationship between the number and form of mitochondria and the physiological state of the cell. Consistent with her report, there were only one to four mitochondria in exponentially growing glucose-repressed cells (Table 1 and Fig. 5). Also, mitochondria occupied <2% of cell volume and mitochondrial cristae were not developed in our culture condition (Table 2 and Fig. 1c).

Comparison with *E. dermatitidis* structome

We have previously reported the structome of *E. dermatitidis*, an ascomycetous black yeast, in the G1 phase [8], making it possible to compare structomes between *S. cerevisiae* and *E. dermatitidis*.

There were no lipid bodies, glycogen granules, nor storage materials in *S. cerevisiae*, whereas these components were present in *E. dermatitidis*. On the other hand, there were small vesicles, filasomes, peroxisomes, and virus-like particles in *S. cerevisiae*, whereas these components were not present in *E. dermatitidis*. There were fewer mitochondria in *S. cerevisiae* than in *E. dermatitidis* (1–4 vs. 17–52). Also, the volume of mitochondria in *S. cerevisiae* was much less than that of *E. dermatitidis* (<2% against 10% in *E. dermatitidis*). The proportion of cytosol in *S. cerevisiae* was greater than that in *E. dermatitidis* (64 vs. 48%). It requires more information on structomes of other cells to understand what these differences between *S. cerevisiae* and *E. dermatitidis* mean.

Future studies

It may be interesting to collect detailed structural information (structome) on cells in different cell cycles (see above) and grown in different culture conditions. Also, studying the structome of various other cell types such as animal cells, plant cells, fungal cells and tissue culture cells would prove to be interesting, although these may be technically difficult.

In this study, we used *S. cerevisiae* S288c strain since genome information of this strain is already available. In order to understand the mechanisms of life, we need to know how genes control protein synthesis through RNA transcription and how protein products are transported to the right place in a cell. Structomes will become more important if localization of each protein can be determined using specific tags. A genetically encoded tag analogous to green fluorescent protein could enable identification of specific proteins in ultrathin sections by electron microscopy. Attempts toward this end are now in progress [26].

Other means for structome analysis than serial ultrathin sectioning

Serial ultrathin sectioning of whole cells is technically very difficult. Recently, other means to analyze 3D cell structure has been reported, namely electron tomography [25,27,28], serial block-face scanning electron microscopy [29], soft X-ray tomography [30] and X-ray diffraction microscopy [31]. Although these new approaches are very useful, resolution of images are inferior to electron microscopy of ultrathin sections. Improvement of resolution of images obtained using these methods should come about in the future. Further, attempts have been made to make 3D structural information of the cell publicly available through the Cell Centered Database [32]. A similar database on structome of various types of cells and cell conditions should prove useful for understanding the cell function.

Concluding remarks

Genome is the whole genetic information of an organism; proteome is the whole protein information of a cell or an organism. Similarly,

structome is the whole structural information of a cell at the electron microscopic level, an important concept for understanding the cell function [1]. The concept of structome includes information on individual protein positions within the cell which, we hope, will become possible in the future.

Supplementary data

Supplementary data are available at http://jmicro.oxfordjournals.org/.

Funding

This study was supported by the Ministry of Education, Culture, Sports, Science and Technology of the Japanese Government (19570053).

Acknowledgement

We sincerely thank Dr. Masako Osumi of the Integrated Imaging Research Support and Dr. Tomoko Takagi of Japan Woman's University for valuable discussion.

References

1 Yamaguchi M (2006) Structome of *Exophiala* yeast cells determined by freeze-substitution and serial ultrathin sectioning electron microscopy. *Curr. Trends Microbiol.* **2**: 1–12.

2 Keddie F M and Barajas L (1969) Three-dimensional reconstruction of *Pityrosporum* yeast cells based on serial section electron microscopy. *J. Ultrastruct. Res.* **29**: 260–275.

3 Hoffmann H P and Avers C J (1973) Mitochondrion of yeast: ultrastructural evidence for one giant, branched organelle per cell. *Science* **181**: 749–51.

4 Baba M, Baba N, Ohsumi Y, Kanaya K, and Osumi M (1989) Three-dimensional analysis of morphogenesis induced by mating pheromone alpha factor in *Saccharomyces cerevisiae*. *J. Cell Sci.* **94**: 207–216.

5 Kanbe T, Kobayashi I, and Tanaka K (1989) Dynamics of cytoplasmic organelles in the cell cycle of the fission yeast *Schizosaccharomyces pombe*: three-dimensional reconstruction from serial sections. *J. Cell Sci.* **94**: 647–656.

6 Winey M, Mamay C L, O'Toole E T, Mastronarde D N, Giddings T H, Jr, McDonald K L, and McIntosh J R (1995) Three-dimensional ultrastructural analysis of the *Saccharomyces cerevisiae* mitotic spindle. *J. Cell Biol.* **129**: 1601–1615.

7 Takagi T, Ishijima S A, Ochi H, and Osumi M (2003) Ultrastructure and behavior of actin cytoskeleton during cell wall formation in the fission yeast *Schizosaccharomyces pombe*. *J. Electron Microsc.* **52**: 161–174.

8 Biswas S K, Yamaguchi M, Naoe N, Takashima T, and Takeo K (2003) Quantitative three-dimensional structural analysis of *Exophiala dermatitidis* yeast cells by freeze-substitution and serial ultrathin sectioning. *J. Electron Microsc.* **52**: 133–143.

9 Goffeau A, Barrell B G, Bussey H, Davis R W, Dujon B, Feldmann H, Galibert F, Hoheisel J D, Jacq C, Johnston M, Louis E J, Mewes H W, Murakami Y, Philippsen P, Tettelin H, and Oliver S G (1996) Life with 6000 genes. *Science*. **274** 546, 563–567.

10 Yamaguchi M, Okada H, and Namiki Y (2009) Smart specimen preparation for freeze-substitution and serial ultrathin sectioning of yeast cells. *J. Electron Microsc.* **58**: 261–266.

11 Yamaguchi M, Shimizu M, Yamaguchi T, Ohkusu M, and Kawamoto S (2005) Repeated use of uranyl acetate solution for section staining in transmission electron microscopy. *Plant Morphol.* **17**: 57–59.

12 Stevens J B (1977) Variation in number and volume of the mitochondria in yeast according to growth conditions. A study based on serial sectioning and computer graphics reconstruction. *Biol. Cell.* **28**: 37–56.

13 Zlotonik H, Fernandez M P, Bowers B, and Cabib E (1984) *Saccharomyces cerevisiae* mannoproteins form an external cell wall layer that determines wall porosity. *J. Bacteriol.* **159**: 1018–1026.

14 Schreuder M P, Mooren A T A, Toschka H Y, Verrips C T, and Klis F M (1996) Immobilizing proteins on the surface of yeast cells. *Trends Biotechol.* **14**: 115–120.

15 Yamaguchi M, Miyatsu Y, Mizokami H, Matsuoka L, and Takeo K (1996) Translocation of hepatitis B virus core particles through nuclear pores in transformed yeast cells. *J. Electron Microsc.* **45**: 321–324.

16 Rossanese O W, Soderholm J, Bevis B J, Sears I B, O'Connor J, Williamson E K, and Glick B S (1999) Golgi structure correlates with transitional endoplasmic reticulum organization in *Pichia pastoris* and *Saccharomyces cerevisiae*. *J. Cell Biol.* **145**: 69–81.

17 Baba M, Takeshige K, Baba N, and Ohsumi Y (1994) Ultrastructural analysis of the autophagic process in yeast: detection of autophagosomes and their characterization. *J. Cell Biol.* **124**: 903–913.

18 Hoch H C and Howard R J (1980) Ultrastructure of freeze-substituted hyphae of the basidiomycete *Laetisaria arvalis*. *Protoplasma* **103**: 281–297.

19 Baba M and Osumi M (1987) Transmission and scanning electron microscopic examination of intracellular organelles in freeze-substituted *Kloeckera* and *Saccharomyces cerevisiae* yeast cells. *J. Electron Microsc. Tech.* **5**: 249–261.

20 Matile P, Cortat M, Wiemken A, and Frey-Wyssling A (1971) Isolation of glucanase-containing particles from budding *Saccharomyces cerevisiae*. *Proc. Nat. Acad. Sci. USA* **68**: 636–640.

21 O'Toole E T, Winey M, and Mcintosh J R (1999) High-voltage electron tomography of spindle pole bodies and early mitotic spindles in the yeast *Saccharomyces cerevisiae*. *Mol. Biol. Cell* **10**: 2017–2031.

22 Osumi M, Miwa N, Teranishi Y, Tanaka A, and Fukui S (1974) Ultrastructure of *Candida* yeasts grown on *n*-alkanes. Appearance of microbodies and its relationship to high catalase activity. *Arch. Microbiol.* **99**: 181–201.

23 Herring A J and Bevan E A (1974) Virus-like particles associated with the double-stranded RNA species found in killer and sensitive strains of the yeast *Saccharomyces cerevisiae*. *J. Gen. Virol.* **22**: 387–394.

24 Garfinkel D J, Boeke J D, and Fink G R (1985) Ty element transposition: reverse transcriptase and virus-like particles. *Cell* **42**: 507–517.

25 Noske A B, Costin A J, Morgan G P, and Marsh B J (2008) Expedited approaches to whole cell electron tomography and organelle mark-up in situ in high-pressure frozen pancreatic islets. *J. Struct. Biol.* **161**: 298–313.

26 Nishino Y, Yasunaga T, and Miyazawa A (2007) A genetically encoded metallothionein tag enabling efficient protein detection by electron microscopy. *J. Electron Microsc.* **56**: 93–101.

27 Henderson G P, Gan L, and Jensen G J (2007) 3-D ultrastructure of *O. tauri*: electron cryotomography of an entire eukaryotic cell. *PLoS. ONE* **2**: e749.

28 Koning R I and Koster A J (2009) Cryo-electron tomography in biology and medicine. *Ann. Anat.* **191**: 427–445.

29 Denk W and Horstmann H (2004) Serial block-face scanning electron microscopy to reconstruct three-dimensional tissue nanostructure. *PLoS biology* **2**: e329.

30 Uchida M, Sun Y, McDermott G, Knoechel C, Le Gros M A, Parkinson D, Drubin D G, and Larabell C A (2011) Quantitative analysis of yeast internal architecture using soft X-ray tomography. *Yeast* **28**: 227–236.

31 Jiang H, Song C, Chen C-C, Xu R, Raines K S, Fahimian B P, Lu C-H, Lee T-K, Nakashima A, Urano J, Ishikawa T, Tamanoi F, and Miao J (2010) Quantitative 3D imaging of whole, unstained cells by using X-ray diffraction microscopy. *Proc. Natl. Acad. Sci. USA* **107**: 11234–11239.

32 Martone M E, Tran J, Wong W W, Sargis J, Fong L, Larson S, Lamont S P, Gupta A, and Ellisman M H (2008) The cell centered database project: an update on building community resources for managing and sharing 3D imaging data. *J. Struct. Biol.* **161**: 220–231.

Appendix

In the analysis of the data in Table 6, we assumed, as the null hypothesis, that the vesicles (points) are distributed uniformly inside a cell (an ellipsoid)

$$\frac{x^2}{a^2}+\frac{y^2}{b^2}+\frac{z^2}{c^2}=1 \qquad (1)$$

where $a = 1790$ nm and $b = c = 1485$ nm, the values of a, b and c being those obtained from our experiments. This uniform distribution can be obtained from the uniform distribution inside the cube $V = [-a, a] \times [-b, b] \times [-c, c]$. More specifically, if we let R_x, R_y and R_z be uniform random numbers on the intervals $[-a, a]$, $[-b, b]$ and $[-c, c]$ respectively, then (R_x, R_y, R_z) is a random vector distributed uniformly inside V. The random vector $(X, Y, Z) = (R_x, R_y, R_z)$, satisfying that

$$\frac{R_x^2}{a^2}+\frac{R_y^2}{b^2}+\frac{R_z^2}{c^2}\le 1 \qquad (2)$$

will be distributed uniformly inside the ellipsoid (1). In our analysis, we generated 20 000 points inside V and found that there were 10 418 points satisfying (2).

What we did next is to project the 10 418 points onto the (x, y) plane. The projected points (X, Y) are distributed inside the ellipse

$$\frac{x^2}{a^2}+\frac{y^2}{b^2}=1 \qquad (3)$$

Note that our data were obtained by projecting the points onto the (x, y) plane and measuring the distances from the projected points to the circumference of the ellipse (3). Similarly, we computed the distances PQ from each of the 10 418 projected points P (X, Y) to the circumference of the ellipse (3). Note that if we write the coordinates of Q as Q $(a \cos\theta, b \sin\theta)$, then θ is a solution to the following equation:

$$(bY - b^2 \sin\theta)\cos\theta - (aX - a^2\cos\theta)\sin\theta = 0 \qquad (4)$$

Since there is no analytical formula available for the nonlinear equation (4), we therefore resorted to Newton's method to find numerical solutions to this equation. The empirical distribution of the resulting distances PQ is shown in Fig. A1.

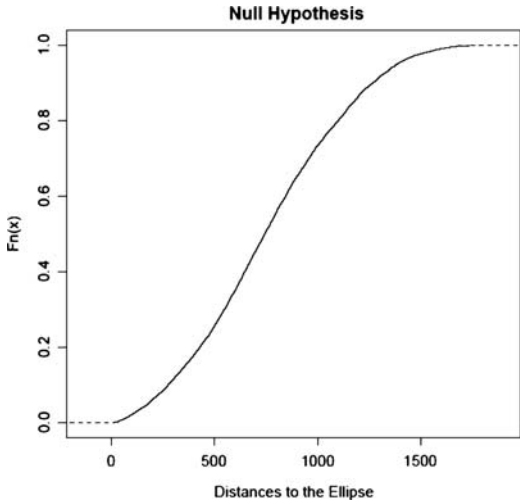

Figure A1 A total of 10 418 points were generated from the uniform distribution inside the ellipsoid (1) and then projected to the (x, y) plane. The figure shows the empirical distribution of the distances from the projected points to the circumference of the ellipse (3).

The empirical distribution of the 45 data points, on the other hand, is shown in Fig. A2. The

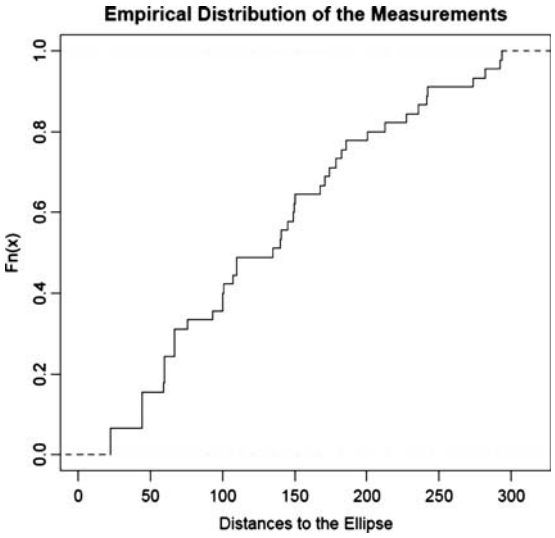

Figure A2 The empirical distribution of the 45 observations.

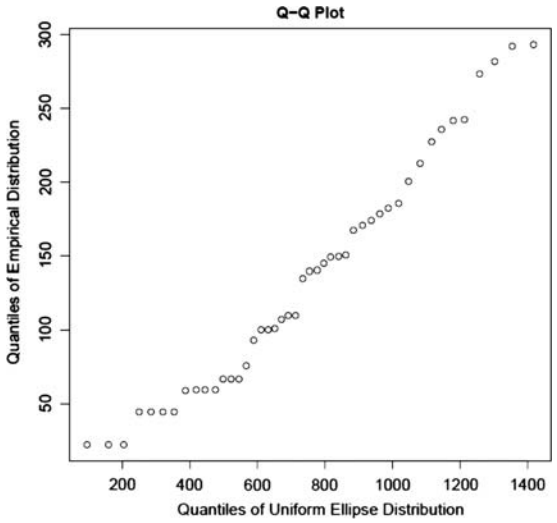

Figure A3 Q–Q plot. Horizontal axis: the quantiles of the empirical distribution of the distances shown in Fig. A1; vertical axis; quantiles of the empirical distribution of the 45 observations.

discrepancy between the two distributions displayed in Figs. A1 and A2 was confirmed by the Q–Q plot shown in Fig. A3. Since the Q–Q plot is far from an idealized straight line, we therefore visually reject the null hypothesis that the points are distributed uniformly inside the ellipsoid (1).

We also applied the Kolmogorov–Smirnov test (KS test; Conover W J: Practical Nonparametric Statistics, New York, John Wiley & Sons, 1971) to the two distributions displayed in Figs. A1 and A2. The KS test is based on the statistic

$$D = \sup_x |F_n(x) - F(x)| \tag{5}$$

where $F_n(x)$ is the empirical distribution of the 45 observations (Fig. A2) and $F(x)$ is the empirical distribution of the distances PQ (Fig. A1) and is derived from the null hypothesis that the points are distributed inside the ellipsoid (1). The observed value of the KS test statistic is $D = 0.8886$, with the corresponding P-value being $<2.2 \times 10^{-16}$. Therefore, the null hypothesis is again rejected by the KS test. Thus, we conclude from our analysis that the vesicles (points) are distributed in a manner significantly different from uniformity inside the cell (ellipsoid) (1).